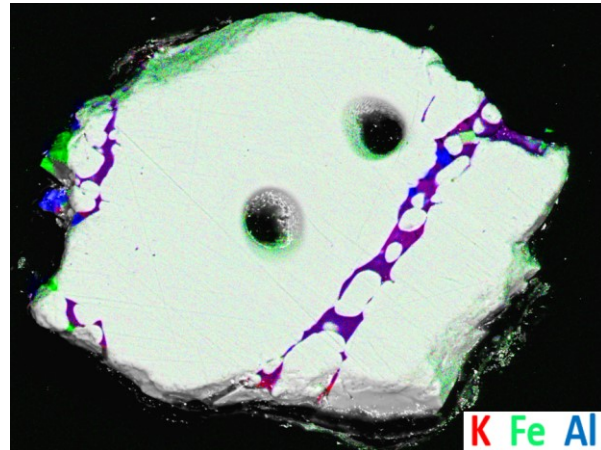


**IMPACT MELT INCLUSIONS IN APOLLO ZIRCONS: TARGET LITHOLOGY TRACERS?** C. Tong<sup>1</sup>, C. Crow<sup>1</sup>, A. Bell<sup>1</sup>, N. Kelly<sup>1</sup>, and D. Moser<sup>2</sup>; <sup>1</sup>University of Colorado Boulder (cyntong2@gmail.com), <sup>2</sup>Bruker, <sup>3</sup>Zircon and Accessory Phase Laboratory, University of Western Ontario

**Introduction:** The crystal structure of zircons has shown to be a good recorder of high shock pressure environments such as meteorite impacts [1-2]. One of the microstructures of interest are entrained melt inclusions produced by shock heating of adjacent minerals that melt and become trapped along shock microstructures in the zircon. Previous work on terrestrial zircons from the Vredefort Impact Structure in South Africa demonstrated that impact melt inclusions are heterogeneous within a single grain and record the composition of the minerals residing near the zircons at time of impact [2]. On the Moon, nearly all zircons and detrital and may preserve evidence of multiple impact events. Impact-derived melt inclusions may provide a unique opportunity to reconstruct the petrogenesis of lunar zircons and contextualize the lunar impact history recorded in Apollo zircons. This project is designed to test if lunar zircon melt inclusions represent current host rocks, or, instead, retain evidence of previous host lithologies.

**Sample:** 14311 is an impact melt breccia which was chosen for this project for its relatively high abundance of zircon and apatite grains. Previous work by Crow et al. [3] identified three different age populations within 14311 zircons ( $4334 \pm 10$ ,  $4245 \pm 10$ , and  $3953 \pm 10$  Ma). They presented a survey of 14311 zircon melt inclusion and observed multiple melt compositions within and between individual zircons.

**Methods:** We collected two datasets, micro x-ray fluorescence (Micro-XRF) and electron microprobe (EPMA) energy dispersive spectroscopy (EDS), for four thick sections of 14311 analyzed by [3]. Micro-XRF data were used to characterize the sample bulk composition and to identify clast and melt components. Wave dispersive spectroscopy (WDS) data of individual mineral grains were then obtained to investigate compositional variations between different lithologies in 14311 for comparison with melt inclusion analyses of Crow et al. [4].



**Fig. 1:** EDS map of Apollo 14311 zircon showing a melt vein enriched in K and Al. Note the spatial variation within the vein. Dark spots in host zircon are SIMS analysis spots.

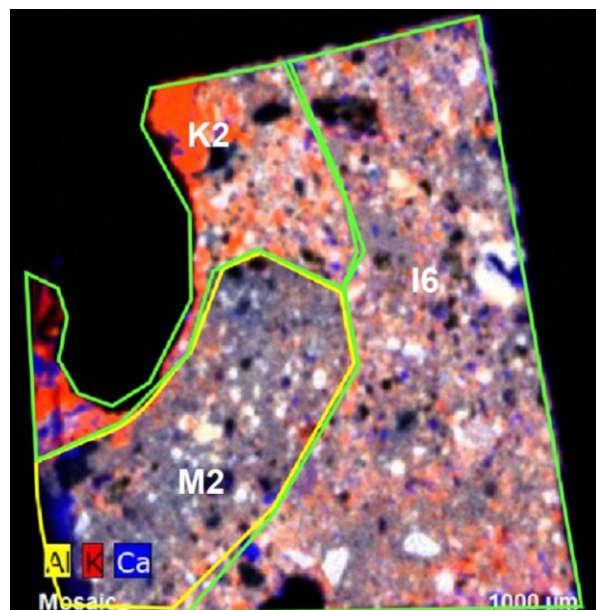


**Fig. 2:** Example micro-XRF map of Al-K-Ca compositions for 14311 thick section (ts3). K=Potassium-rich matrix; I=Intermediately potassium-rich matrix; R(M in this figure)=Potassium-poor matrix.

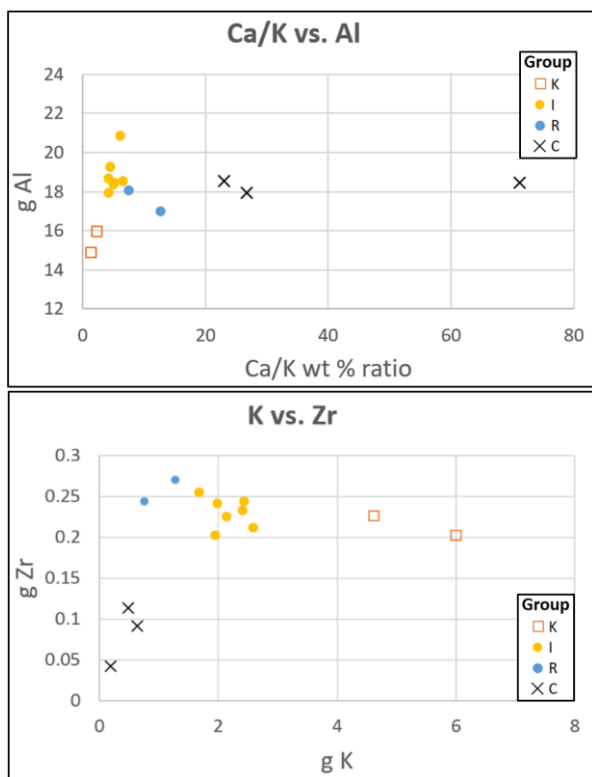


**Figure 3:** Pots of calcium, potassium, and aluminum compositions using micro-XRF data. (A) Calcium-Potassium wt. % ratios vs. Mass aluminum (B) Mass potassium vs. Mass zirconium

**Results:** Micro-XRF data was used to distinguish multiple clast and melt components with a range of potassium content leading to the following classification scheme: K-rich matrix (K), Intermediately K-rich matrix (I), K-poor “regular” matrix (R), and clasts (C) (Fig. 2). Group K is anomalously rich in potassium by 2-4 wt. % over all other groups, while Group C is distinctly Ca-rich and Zr-poor, suggesting the clasts’ protoliths were zircon-poor (Fig. 3). Groups I and R are compositionally similar, with R being marginally less potassic and aluminous.

These classifications are further supported by feldspar EMPA data (Fig. 4). Group K represents one end-member with abundant alkali feldspars as well as highly potassic glassy melt. Clasts represent another end-member with feldspars near pure anorthosite composition. Group R plagioclases contains feldspars of both compositions, suggesting mixing between or with other lithologies within the breccia.

Pyroxenes show three distinct compositions (Fig. 5). Clasts were observed to contain magnesium-rich orthopyroxenes. Groups R and K orthopyroxenes and clinopyroxenes are marginally more iron-rich than the clasts. Group I clinopyroxenes are notably iron-rich.

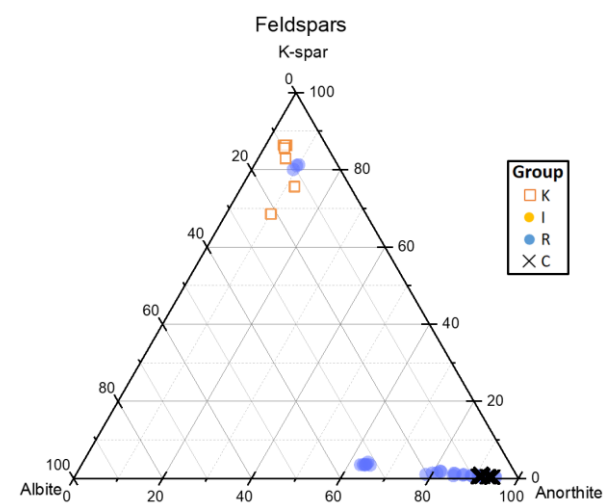


**Figure 4:** Feldspar ternary of EMPA data.

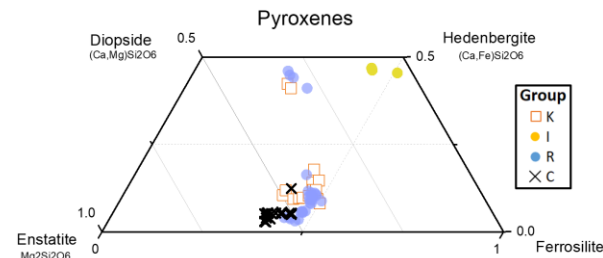


**Figure 5:** Pyroxene quadrilateral of EMPA data.

**Ongoing Work:** Quantitative data acquisition on the melt inclusions is ongoing at ZAP Lab and will be mapped directly against the micro-XRF and EMPA datasets to determine the possible melt sources. However, the abundance high-K melt inclusions observed by [4] in 14311 zircons suggests that these melts may have been entrained while in contact with Group K or Group R lithologies. We aim to conduct a more complete comparison of melt inclusions and nearest-neighbor mineral grains on in-situ zircons in different mineral settings in future polished sections. The compositional results will be synthesized with zircon ages to contextualize the impact history recorded in this impact melt breccia.

**References:** [1] Moser D. E. et al. (2011) *Canadian Journal ES*, 48, 117–139. [2] Davis C.L. (2016) *Electronic Thesis and Dissertation Repository*, 4185. [3] Hopkins M.D. and Mojzsis S.J. (2015) *Contrib Mineral Petro* 169:30. [4] Crow C. A. et al. (2019) *LPS L*, Abstract #2023.